Int J Earth Sci (2000) 89 : 350–365

ORIGINAL PAPER

T. Doutsos · I. Koukouvelas · G. Poulimenos
S. Kokkalas · P. Xypolias · K. Skourlis

An exhumation model of the south Peloponnesus, Greece

Received: 16 April 1999 / Accepted: 19 January 2000

Abstract An exhumation model comprising forward and backward thrusting and late orogenic collapse is proposed in order to explain the kinematics of the tectonic windows in the south Peloponnesus. The model is based on mapping, mesoscopic structural data and strain analysis. Syn-compressional thickening took place throughout the Oligocene and Early Miocene which includes the subduction of the Pindos Ocean at the western margin of the Pelagonian microcontinent and the intracontinental subduction of the Phyllite–Quartzite and the Plattenkalk series. The latter subduction was associated with blueschist metamorphism, westward-directed ductile thrusting, and folding. The exhumation history of the deeper parts of the orogen began at the Oligocene–Miocene boundary with the progressive entrance of the low-density crust and the Plattenkalk carbonates in the subduction zone. Increased buoyancy caused: (a) the initiation of the Phyllite–Quartzite series extrusion; (b) vertical coaxial stretching; and (c) the evolution of two pop-up structures, i.e. the Parnon and Taygetos anticlines. This syn-compressional exhumation was taking place in the lower Miocene with decreasing rates from 7 to 1.5 mm/year. The change in the local stress field from compression to extension began in the middle Miocene with the formation of hinterland-dipping normal faults. The exhumation/denudation rate caused by the footwall uplift along these faults does not exceed 0.2 mm/year.

Key words Syncompressional uplift · Synextensional uplift · Tectonic windows · Greece

T. Doutsos (✉) · I. Koukouvelas · G. Poulimenos · S. Kokkalas
P. Xypolias · K. Skourlis
Department of Geology, University of Patras, GR-26500 Patras, Greece
e-mail: tdoutsos@upatras.gr
Tel.: +30-61-997843
Fax: +30-61-994485

Introduction

Since the work of Suess (1904) who first described tectonic windows as the lower parts of orogenic belts below flat-lying tectonic contacts, the origin of these structures has remained highly problematic. Highlighted by Wunderlich (1966), the main question is: Why is erosion confined, especially in the axial zones of orogenic belts, just in the locations of the future windows? Strong uplift, responsible for this intensive erosion, has been attributed to several mechanisms. The classical mechanism of "syncompressional uplift and erosion" comprises intracontinental folding and thrusting (Hsu 1991) caused by the underplating of one or two converging plates, with resultant forward and/or backward thrusting ("retrocharriage"), respectively. Recent papers, supporting this mechanism in the Alps, emphasize the role of vertical and/or horizontal extrusion of highly strained ductile zones in the internal parts of this orogenic belt (Merle and Guillier 1989; Ratschbacher et al. 1991; Ring 1992). However, syncompressional uplift and erosion, as a unique exhumation mechanism, is unable to explain the relatively thin deposits of flysch and molasse preserved within the syn- to late orogenic basins of many orogenic belts (Platt 1986). Another group of mechanisms that explain the exhumation of rocks formed at deep structural levels includes tectonic denudation by normal faulting, often associated with footwall uplift and erosion (Davis and Coney 1979; Lister et al. 1984; Wernicke et al. 1988). In these models, extension is the direct result of collapse of a thickened buoyant crust during or after plate convergence (Platt 1986; Dewey 1988; Burchfiel and Royden 1985).

Presently, most authors believe that both mechanisms, syncompressional uplift followed by tectonic denudation and normal faulting, contribute to the formation of tectonic windows. However, it is often very difficult to distinguish between contractional and extensional structures within the highly strained meta-

morphic rocks in the core of the windows, as well as to determine the time of superposition of these structures (e.g. Wallis et al. 1993). Much current research therefore focuses on the question: "To what degree do these mechanisms contribute to the uplift history of an orogen?".

We concentrated our studies on the south Peloponnesian windows (Taygetos, Parnon; Fig. 1). These windows comprise rocks that originally formed the northeastern margin of the Apulian microcontinent, which moved northeastwards during the early Tertiary towards the Hellenic subduction zone and subsequently collided with several European microplates (Doutsos et al. 1993; Doutsos et al. 1994). These windows contain some of the youngest blueschist rocks in the world, with metamorphism geochronologically dated at approximately 24 Ma (Panagos et al. 1979; Seidel et al. 1982). The geological structures within the windows are very well preserved. Furthermore, excellent stratigraphic data from within the synorogenic basins surrounding the blueschists (Aubouin 1959; Richter 1976; Bizon and Thiebault 1974; Kowalczyk et al. 1977) are available. These data can be combined with our structural analysis and allows us to propose an exhumation model comprising forward and backward thrusting, and late orogenic collapse. In addition, an attempt is made to quantify the exhumation/denudation history of the tectonic windows and to distinguish between the syncompressional and synextensional components of exhumation/denudation. We use the terms "uplift", as the vertical motion of the surface with respect to a fixed reference level, and "exhumation", as the vertical motion of rocks with respect to the surface, according to England and Molnar (1990). The term "denudation" is used when material is removed from the earth's surface either by erosion or by tectonic activity.

Tectonic setting of south Peloponnesus

The Apulian microcontinent in the Peloponnesus constituted a carbonate platform during the early Mesozoic, which later in the late Jurassic was subdivided by rifting into deep basins and shallow ridges forming the classic isopic zones of the External Hellenides (Philippson 1892; Aubouin 1959; Bernoulli and Renz 1970). During this time two shallow-water platform areas, the Tripolitsa and Pre-Apulian zones, became separated by the Ionian zone (Fig. 1), a deep-water basin filled with thin limestones and cherts (Karakitsios 1995). To the east the Tripolitsa zone passed gradually into a thin pelagic sequence of cherty limestones and radiolarites, known as "the Pindos zone", which formed the passive continental margin flanking the Pindos Ocean which lay to the east (Clift 1992). During an early Tertiary tectonic inversion the "mobile" parts of this platform, the Pindos and Ionian zones, were detached from an unknown basement and thrust westwards onto the stable Tripolitsa zone and the Pre-Apulian zone, respectively (Fig. 1a; Jacobshagen et al. 1978). The base of the Tripolitsa zone is exposed in several tectonic windows in the central and south Peloponnesus and comprises the Phyllite–Quartzite series (PQ). The PQ series comprises phyllites with carbonate intercalations, quartzites, metaconglomerates, anhydrites and basic to intermediate metavolcanics. The upper part of this series, known as the "Tyros beds" (Ktenas 1924), contains fossils ranging from Permian (Fytrolakis 1971; Lallemant 1984) to Upper Triassic in age (Doert et al. 1985) implying stratigraphic continuity with the base of the Upper Triassic Tripolitsa limestones (Thiebault and Zaninetti 1974). The protolith of the PQ series may have been a Permian–middle Triassic rift sequence (Thiebault 1982) which can be compared with middle-Triassic rift sequences in the Dinarides (Brauer 1983). The Tyros beds of the PQ series were metamorphosed at 240–350 °C and 3–6 kbar (Seidel 1978; Thiebault and Triboulet 1984). In the rest of the PQ series the occurrence of garnet, glaucophane and chloritoid (Paraskevopoulos 1964; Katagas 1980; Pe-Piper 1982) indicates considerably higher P–T conditions. Maximum P–T conditions of this metamorphism have been estimated at 350–450 °C and 11–13 kbar by Theye (1988) or 450–550 °C and 17 kbar by Theye and Seidel (1991). Published pressure–temperature–time paths for the PQ series in Peloponnesus, Kythira and western Crete (Fig. 1) are presented in Fig. 2.

The PQ series was tectonically emplaced by the Taygetos and Parnon thrusts on the Plattenkalk series (PLK), which is the deepest structural unit in the Peloponnesus. The PLK series comprises a neritic sequence of Upper Triassic in age (Tataris and Maragoudakis 1970) overlain by pelagic carbonate rocks of Jurassic to Upper Eocene age (Thiebault 1982; Blumor 1998). Resting conformably on these Mesozoic carbonates is a flysch sequence of lower Oligocene age (Bizon and Thiebault 1974; Kowalczyk and Zugel 1997) and beneath the carbonate rocks (only in the Taygetos area) are the Kastania phyllites (Psonis 1981; Dittmar and Kowalczyk 1989) which are probably of Permo-Triassic age. Recrystallized quartz and synkinematic growth of chloritoid in the PLK carbonate rocks of Taygetos Mountain area indicate P–T conditions at the Anchizone/Epizone boundary (Manutsoglu 1990). The occurrence of (Fe–Mg) carpholite, having an Fe–Mg composition ranging from 0.48 to 0.51 and the mineral paragenesis carpholite+chlorite+pyrophyllite+quartz within the Kastania phyllites indicate high-pressure/low-temperature (HP/LT) metamorphic conditions of 7–8.5 kbar and 310–360 °C (Blumor et al. 1994). Further east, in the Parnon mountain area, an increase in the grade of metamorphism in the PLK carbonates was recognized (Thiebault 1982) with peak metamorphic conditions estimated at 2–5 kbar and 450–480 °C (Bassias 1989). Comparison of rock types and fossil record have led some authors to postulate

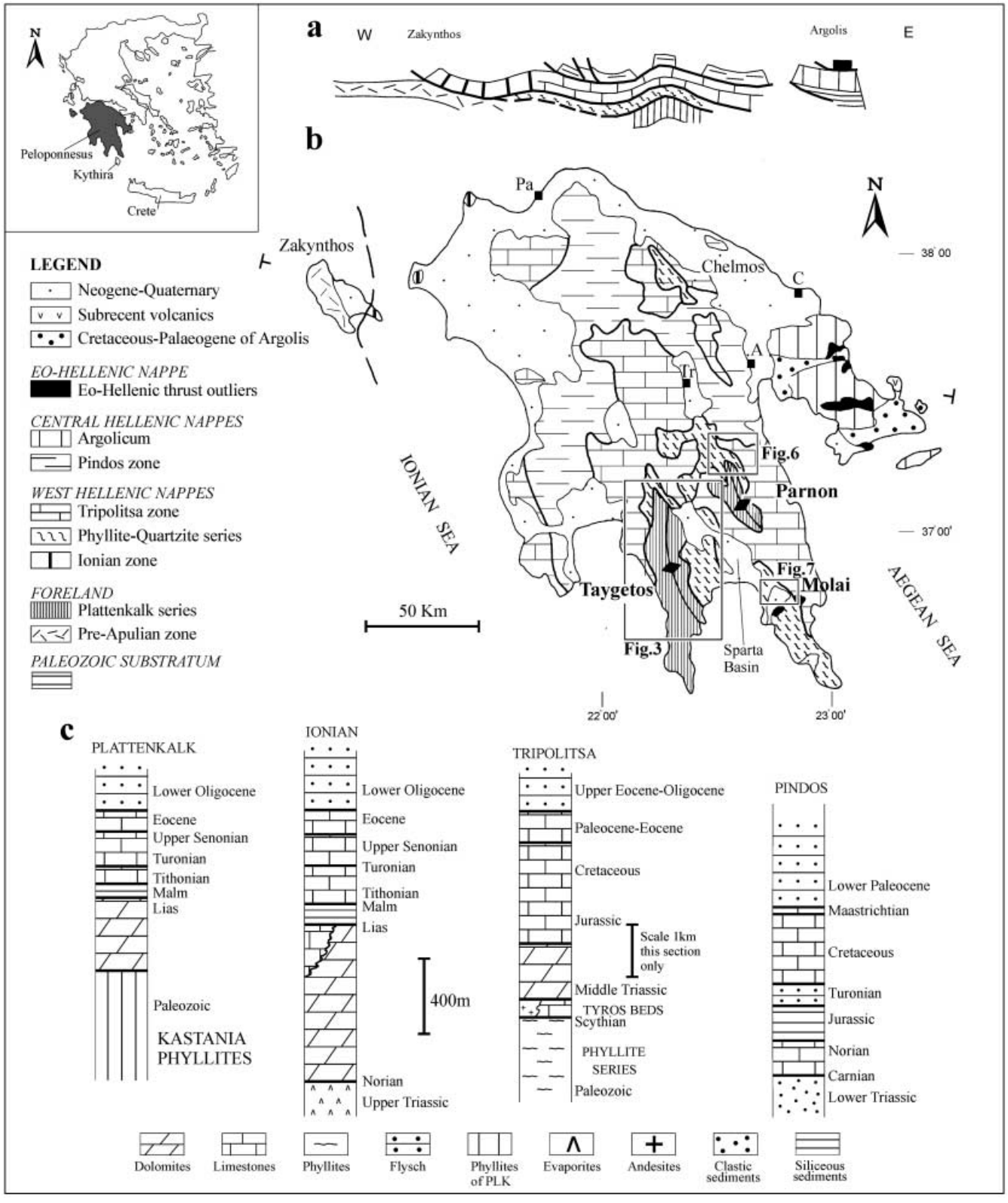

Fig. 1 Schematic cross section defining nappe stacking of the Peloponnesus (after Jacobshagen et al. 1978). **b** General tectonic map of the Peloponnesus (modified after Jacobshagen et al. 1978). Taygetos, Parnon windows and Molai area are in *rectangles*. *Pa* Patras; *C* Corinthos; *A* Argos; *Tr* Tripolis. **c** Lithostratigraphic columns from the Peloponnesus; Plattenkalk series (after Thiebault 1982 and Blumor et al. 1994), Ionian zone (after Thiebault 1982), Tripolitsa zone, Tyros beds and Phyllites–Quartzite series (after Dercourt 1964; Psonis 1981; Brauer 1983), Pindos zone (after Dercourt 1964). *Inset* shows the geographical position of the Peloponnesus

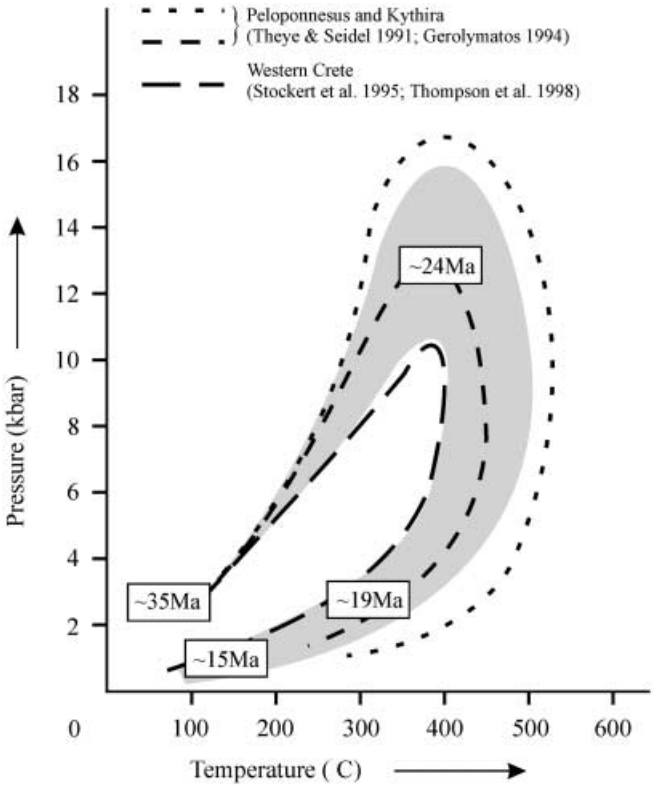

Fig. 2 Combined pressure–temperature–time (P–T–t) paths for the high-pressure/low-temperature rocks of the PQ series in Peloponnesus, Kythira and western Crete. Timing of high-pressure/low-temperature metamorphism after Seidel et al. 1982; all other age data after Thomson et al. 1998

that the PLK series is the southern prolongation of the Ionian zone (Bonneau 1973; Bassias and Thiebault 1985), whereas others (Jacobshagen et al. 1978; Jacobshagen 1994) place the PLK series in a more external position between the Ionian and Pre-Apulian zones.

The Tertiary uplift history of Peloponnesus is very well shown in the stratigraphic record of the syn-orogenic basins. Shortening started in the Pindos zone in the late Eocene and migrated progressively westwards, during the Oligocene and early Miocene (Aubouin 1959). At the Late Eocene–Early Oligocene boundary, the Pindos zone was overthrust westwards onto the eastern parts of the Tripolitsa zone forming the Pindos orogenic belt (Kowalczyk et al. 1977). In the resulting foredeep formed to the west, the west-Hellenic flysch (Jacobshagen 1986) was deposited over the Tripolitsa and Ionian zones, from the lower Oligocene to the middle Miocene (Richter 1976). At the same time, the Pindos zone was successively overthrust to a distance of more than 100 km westward over the west Hellenic flysch (Temple 1968).

In the PLK series, flysch deposition ceased in the middle Oligocene, when these rocks were underplated eastwards to reach HP/LT conditions. Pebbles derived from the PLK series in the extensional basins of Peloponnesus, Kythira (Fig. 1, inset) and Crete (see Kowalczyk et al. 1977; Meulenkamp et al. 1977; Postma and Drinia 1993) indicate that this zone reached the earth's surface in the upper Miocene. The purpose of this paper is to describe and quantify this fast subduction and exhumation history of a young orogen by comparing the structural data collected from the tectonic windows in the south Peloponnesus (Taygetos, Parnon; Fig. 1) with structural data from the adjacent syn- and late orogenic basins.

The Taygetos window

Contractional structures

Structural mapping

The PLK in the core of the Taygetos window forms a NW/SE- to N/S-trending anticline which is more than 60 km long and 15 km wide, called hereafter the "Taygetos anticline" (Fig. 1). It is west verging, convex to the west, and has a flat-lying long limb in the east and a short, steeply dipping overturned limb in the west (Fig. 3, cross section B–B′). The core of this anticline is occupied by the strongly deformed Kastania phyllites, which also form the cores of some second-order anticlines (Fig. 3, cross sections A–A, B–B′, F–F′ and tectonic map). Two west-dipping thrusts (backthrusts, recognized by Psonis 1981) cut the steeply dipping limb of the anticline and carry the base of the Taygetos carbonates or the Kastania phyllites above the Oligocene flysch which conformably overlies the Eocene carbonates at the top of the PLK. Therefore, maximum stratigraphic separation on these thrusts, with lengths ranging between 8 and 15 km, is of the order of 1000 m. Kinematically similar backthrusts, smaller in length and stratigraphic separation, also affect the west dipping short limb of a second-order anticline (Fig. 3, cross section A–A).

In some places, along the western margin of the Taygetos (Fig. 3, cross section C–C′) the multi-coloured carbonates, exposed on the top of the PLK, gravitationally glided over the underlying flysch, and in other places the carbonates are found as olistostromes within the lower clastic deposits of the flysch basin. The contact between the PLK and the surrounding phyllites of the PQ series is marked by cataclasites up to 15 m thick and by protomylonites up to 1 m thick (Fig. 3, cross section C–C′). At the western margin of the window this contact dips gently to the west (Fig. 3, cross section A–A), whereas at the eastern margin its shape is more complex: in the north it dips moderately to the east (Fig. 3, cross section A–A), whereas in the southeast it is overturned and dips steeply to the west (Fig. 3, cross sections B–B′, D–D′ and E–E′).

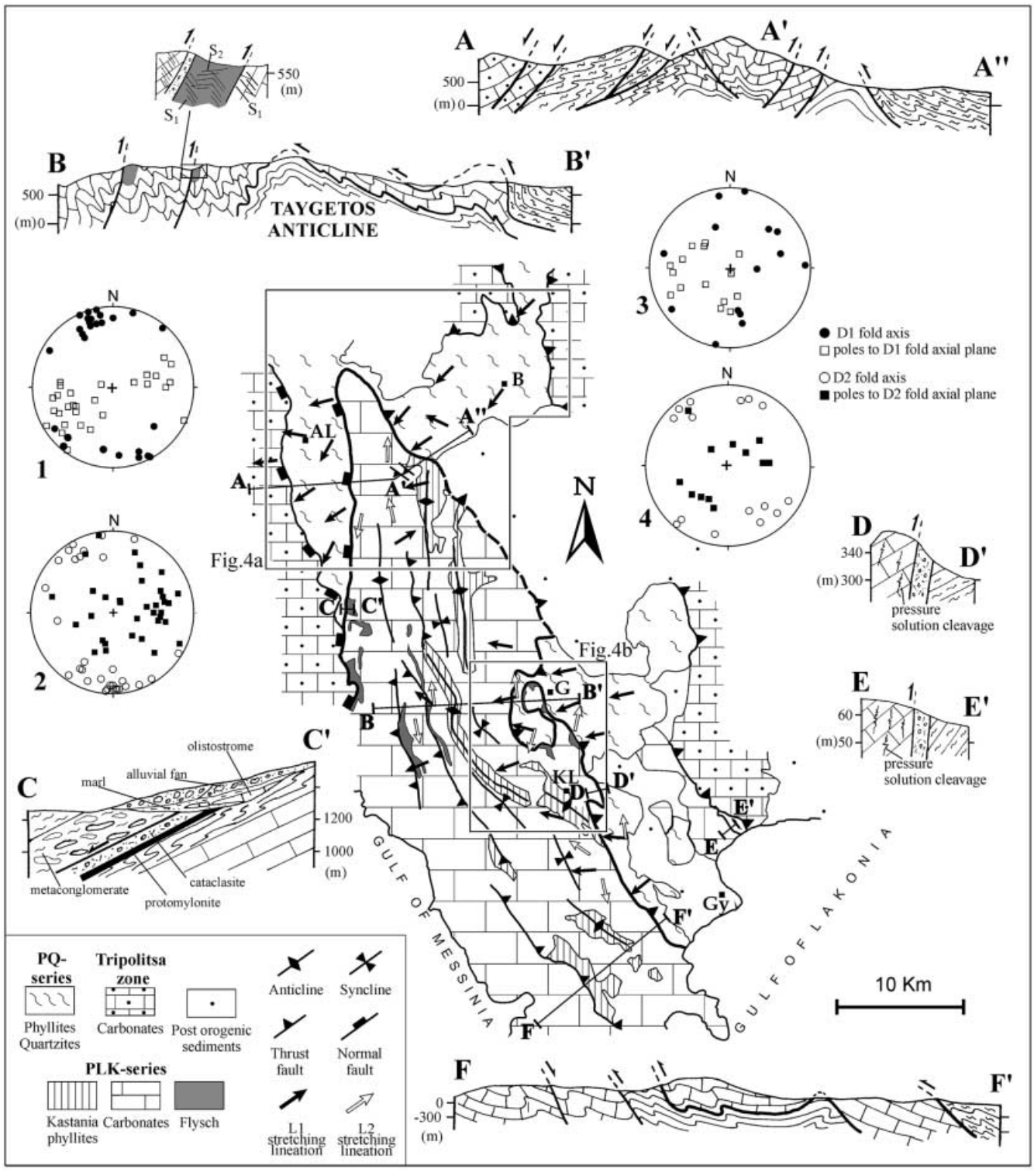

Fig. 3 Tectonic map, cross sections and equal-area projections for D1 and D2 phases of deformation for the Taygetos window. Location of map is given in Fig. 1. *AL* Alagonia; *B* Boutiani; *G* Gorani; *Gy* Gythio

Mesoscopic structures

Deformation at the mesoscopic scale is represented by D1 and D2 structures. D1 folds trend NNW and verge mainly to the west (Fig. 3, net 1). East-verging folds (Fig. 3, net 1) and upright box folds with conjugate axial planes are also common. Folds are tight to isocli-

nal with stretched limbs and have rounded and thickened crests and troughs. A mineral lineation parallel to the trend of the fold axes occurs only in the incompetent marble beds and on the foliation of the Kastania phyllites. Minerals such as chlorite, chloritoid and sericite are aligned parallel to an axial planar schistosity. D1 folds are homoaxially or heteroaxially refolded by D2 folds producing a wide distribution in the stereonet. D2 folds trend NNW to NNE, verge eastwards (Fig. 3, net 2) and are generally associated with a NNE-trending mineral/stretching lineation. They are kink-like in shape and a fracture cleavage or a pressure solution cleavage is developed trending parallel to axial planes.

The southern part of the PLK–PQ contact, at the eastern margin of the window, displays a dense pattern of steeply dipping pressure solution surfaces (Fig. 3, cross sections D–D′ and E–E′) indicating that this contact was reactivated and contracted during the D2 phase.

The most dominant fabric element in the PQ series is a gently dipping foliation consisting of tabular lenticles that comprise remnants of isoclinal folds and strongly elongated boudins. The foliation displays a pervasive WSW-trending stretching lineation (Fig. 3, tectonic map) defined by elongate quartz aggregates, micas and chlorites, showing the direction of the nappe movements. Intrafoliate D1 fold axes show a scatter (Fig. 3, net 3) and tend to become parallel to the stretching lineation. D2 structures include open asymmetric folds, chevron to kink folds with axes and axial planes showing much scatter in stereographic projection (Fig. 3, net 4).

Quartz c-axis fabrics

To determine additional kinematic information from the PQ series, we made a fabric analysis based on the preferred orientation of quartz c-axes. Quartz-rich tectonites commonly develop crystallographic preferred orientation patterns showing geometries that can be useful in assessing the kinematics of deformation events (Lister and Hobbs 1980; Schmid 1982; Simpson and Schmid 1983). The asymmetry of c-axis fabrics with respect to specimen co-ordinates indicates the sense of shear. All selected samples were taken from quartz-rich horizons of the PQ series. No reported samples were collected from discrete shear zones; therefore, the kinematic interpretation is regarded as being valid at least on the scale of the outcrop from which it was taken. Petrofabric analysis of quartz c-axis preferred orientations was made on one X–Z thin section from each sample, cut perpendicular to foliation and parallel to the stretching lineation, measured using an optical microscope and universal stage, along spaced traverses. A general minimum of 200 c-axis measurements was made in each thin section. The c-axis data are displayed on equal-area, lower hemisphere, spherical projections whose plane of projection contains the specimen lineation (X) and pole (Z) to foliation. In all these projections the foliation is vertical and lineation within the foliation is horizontal. The c-axis plots were made using the computer program by R. Allmendinger (Microstructure v.2.5, 1988–1992).

Although approximately 15 oriented samples were collected from the PQ series, only five contained sufficiently quartz-rich domains for a meaningful c-axis fabric analysis to be made. All five samples reveal a distinctly asymmetrical pattern. Quartz c-axis fabrics shown in Fig. 4 (Q1–Q5), with well-developed preferred orientation patterns, display a central girdle segment, which is oblique to the foliation. This obliquity indicates the external asymmetry of the fabric (Platt and Behrmann 1986) with respect to the finite-strain reference frame. It shows a general top-to-the-WSW sense of shear, which is consistent with non-coaxial deformation (Simpson and Schmid 1983; Law 1987). Therefore, the tectonic contact between the PLK and PQ series is probably a thrust (called hereafter Taygetos Thrust) along which PQ series is overthrust westwards onto the PLK. A strong modification of the WSW movement is inferred from sample Q4 (Fig. 4b). This shows a top-to-the-SSW sense of shear, in agreement with strain analysis, suggesting movement in the direction of the L_2 lineation.

The quartz c-axis fabrics in Fig. 4 (Q1–Q5) show no convincing progressive increase in the degree of fabric asymmetry towards the Taygetos Thrust. Our samples show transitional c-axis fabrics varying between an asymmetrical cross-girdle and a variably kinked, single girdle fabric, as the non-coaxial component of the strain path increases (Schmid and Casey 1986). Following the criteria described by Etchecopar and Vasseur (1987), such a pattern indicates approximately plane strain deformation (slightly into the constrictional field).

Finite strain

For finite-strain analysis twenty sites within the PQ series were selected from varying distances perpendicular to the axis of the Taygetos anticline; ten sites were selected from the PLK series (Fig. 4). All the sites are located on the limbs of symmetrical sinusoidal folds, to avoid local strain variation that might have occurred in the hinges. Two mutually perpendicular principal planes, the X–Z and Y–Z planes, were used for each sample, one oriented parallel to the stretching lineation (X) and normal to the foliation, and the other oriented normal to the stretching lineation. Finite-strain values were calculated from shapes of deformed pebbles in metaconglomerates (5 sites), and from detrital quartz grains and quartz aggregates in quartz-rich schists (25 sites), using enlarged photomicrographs of thin sections. The choice of the

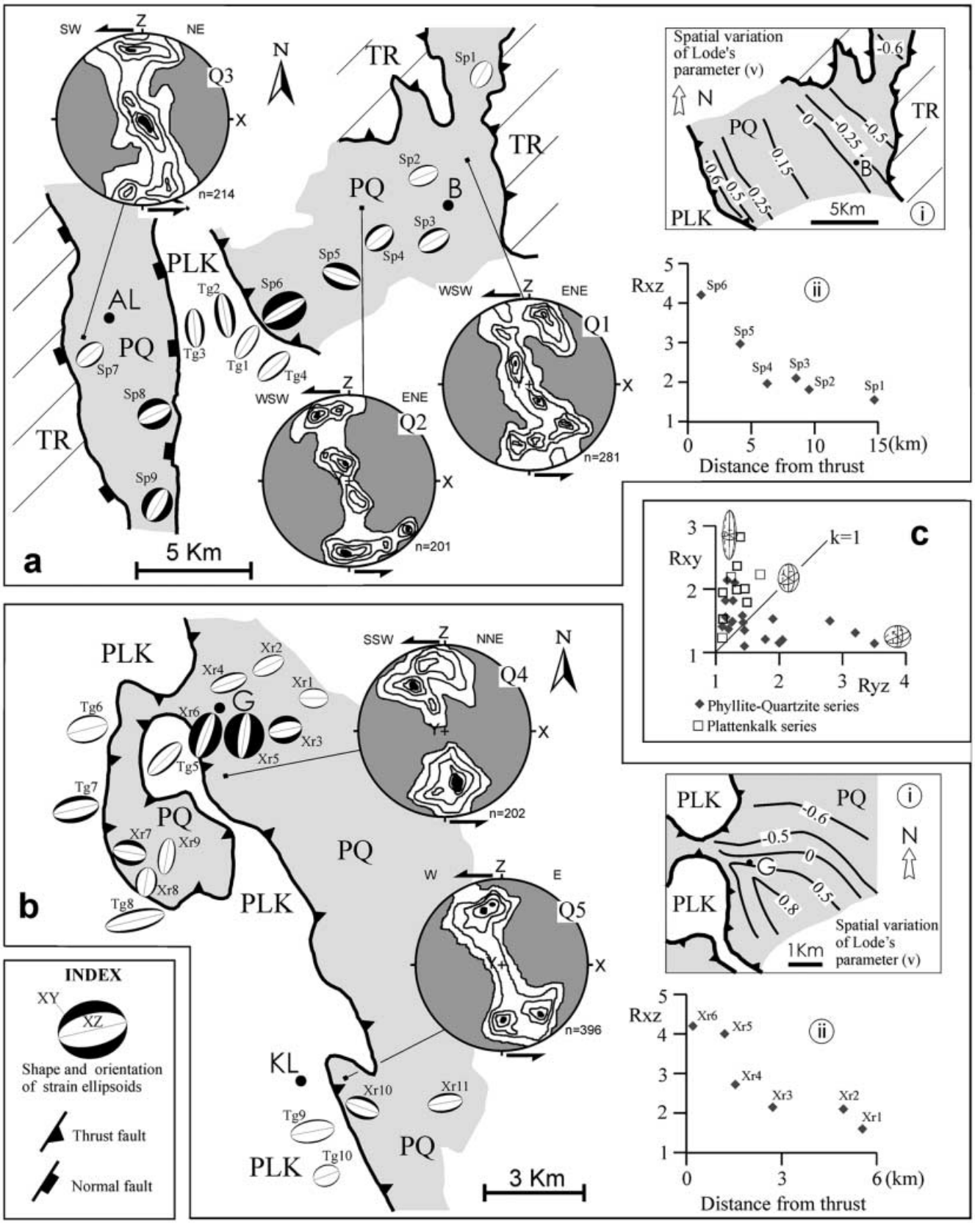
a
SW
NE
Z
X
Q3
n=214
N
TR
Sp1
Sp2
PQ
B
Sp3
Sp4
Sp5
Sp6
PLK
AL
Tg2
Tg3
Tg1
Tg4
Sp7
Sp8
Sp9
TR
WSW
ENE
Q1
n=281
Q2
n=201
5 Km
Spatial variation of Lode's parameter (ν)
-0.6
-0.5
-0.25
0
0.15
0.25
5Km
i
Rxz
ii
Distance from thrust
15(km)
c
Rxy
Ryz
k=1
Phyllite-Quartzite series
Plattenkalk series
b
PLK
Xr2
Xr4
Xr1
Tg6
Xr6
G
Xr3
Xr5
Tg5
Tg7
PQ
Xr7
Xr9
Xr8
Tg8
SSW
NNE
Q4
n=202
W
E
Q5
n=396
KL
Xr10
Xr11
Tg9
Tg10
3 Km
INDEX
XY
XZ
Shape and orientation of strain ellipsoids
Thrust fault
Normal fault
-0.8
1Km
Xr6
Xr5
Xr4
Xr3
Xr2
Xr1
6 (km)

Fig. 4 Strain maps for the **a** northern part and **b** central part of the Taygetos window, showing orientation and shape of finite strain ellipsoids (*XZ* and *XY* sections) and quartz c-axis fabrics (contours at 1% per 1% area with Sp , Tg and *Xr* refer to sample locations. Finite-strain data are given in Table 1. Insets *a(i)* and *b(i)* show spatial variation of Lode's parameter in PQ series in the two parts of the Taygetos window. *a(ii)* and *b(ii)* plots show the variation of *Rxz* values towards the Taygetos thrust. **c** Flinn diagram of the finite strain data. *AL* Alagonia; *B* Boutiani; *G* Gorani; *KL* Kokkina Louria

method of strain analysis was determined by the type of fabric and strain marker. Normalized Fry spatial analysis (Fry 1979; Erslev 1988) was used for detrital quartz grains (Dunne et al. 1990), and R_f/ϕ shape analysis (Ramsay 1967; Dunnet 1969; Lisle 1985) was used for the deformed pebbles (Dunnet 1969) and quartz aggregates (Jensen 1984). The thin sections were analysed and concomitant calculations on photomicrographs were done using the software package INSTRAIN (Erslev 1988; Erslev and Ge 1990). In each case a minimum of 60 objects for the R_f/ϕ method and 150 objects for the normalized Fry method were used. Finally, the strain ellipsoids were calculated from two strain ellipses (Rxz, Ryz) parallel to two principal planes (X–Z and Y–Z planes) using the formula $Rxz = Rxy \times Ryz$, assuming a constant volume ellipsoid (Ramsay and Huber 1983). Thin-section observations indicate that the dominant deformation is intracrystalline plasticity, and thus the constant volume assumption appears to be valid.

The results (Table 1) plotted in a Flinn diagram (Fig. 4c) show that PLK samples systematically differ from PQ samples. PLK samples lie within the apparent constrictional field where deformation produced prolate strain ellipsoids (average value of strain $Rxz = 2.74$), whereas PQ samples lie within both the apparent constrictional field and the apparent flattening field, showing prolate to oblate strain ellipsoids. To define the spatial variations between the two extreme types of strain ellipsoids (prolate–oblate) we constructed two contour maps of Lode's parameter (ν; Hossack 1968; Ramsay and Huber 1983) from two areas within the PQ series (Fig. 4a(i), 4b(i)). The spatial variation of Lode's parameter indicates a gradual increase in ν-value from the east ($\nu = -0.6$, prolate) towards the Taygetos Thrust, where the strain ellipsoid becomes oblate ($\nu = 0.6$). The same strain pattern was observed within the western part of the PQ series near Alagonia village (Fig. 4a). Two locations (Sp8, Sp9) near the Taygetos Thrust showed oblate strain ellipsoids, but further west the prolate shape (Sp7)

Table 1 Finite-strain data. *k* Flinn parameter; *v* Lode's parameter; *dq* detrital quartz; *qa* quartz aggregates; *dp* deformed pebbles

Site	Strain method	Strain markers	Principal axes of finite strain $1+e_1 \geq 1+e_2 \geq 1+e_3$			k	ν
Phyllite–Quartzite series							
Sp1	NFry	dq	1.30	0.92	0.84	4.10	−0.56
Sp2	R_f/φ	qa	1.42	0.90	0.78	3.70	−0.51
Sp3	R_f/φ	qa	1.46	0.98	0.69	1.10	−0.04
Sp4	R_f/φ	qa	1.40	1.03	0.71	0.77	0.10
Sp5	R_f/φ	qa	1.65	1.07	0.57	0.59	0.21
Sp6	R_f/φ	dp	1.76	1.34	0.42	0.14	0.62
Sp7	R_f/φ	qa	1.39	0.95	0.75	1.88	−0.29
Sp8	R_f/φ	dp	1.38	1.20	0.61	0.15	0.66
Sp9	R_f/φ	dp	1.44	1.19	0.58	0.20	0.59
Xr1	R_f/φ	qa	1.33	0.92	0.83	4.50	−0.58
Xr2	R_f/φ	qa	1.56	0.86	0.75	5.46	−0.61
Xr3	R_f/φ	qa	1.35	1.15	0.64	0.27	0.50
Xr4	R_f/φ	qa	1.78	0.85	0.66	3.60	−0.48
Xr5	R_f/φ	dp	1.65	1.44	0.42	0.06	0.81
Xr6	R_f/φ	dp	1.85	1.23	0.44	0.27	0.43
Xr7	R_f/φ	qa	1.40	0.95	0.76	1.92	−0.27
Xr8	R_f/φ	qa	1.30	0.96	0.80	1.85	−0.26
Xr9	NFry	dq	1.75	0.82	0.70	6.30	−0.64
Xr10	R_f/φ	qa	1.53	0.96	0.68	1.38	−0.13
Xr11	R_f/φ	qa	1.62	0.88	0.70	3.03	−0.42
Plattenkalk series							
Tg1	NFry	dq	1.81	0.83	0.67	4.95	−0.56
Tg2	NFry	dq	2.04	0.91	0.54	2.23	−0.20
Tg3	NFry	dq	1.80	0.90	0.61	2.10	−0.28
Tg4	NFry	dq	1.79	0.87	0.67	3.52	−0.46
Tg5	NFry	dq	1.91	0.82	0.63	4.40	−0.52
Tg6	NFry	dq	1.36	0.90	0.79	3.92	−0.52
Tg7	NFry	dq	1.71	0.96	0.62	1.42	−0.13
Tg8	NFry	dq	2.20	0.76	0.59	6.75	−0.61
Tg9	NFry	dq	1.62	0.84	0.75	7.66	−0.70
Tg10	NFry	dq	1.18	0.96	0.88	2.45	−0.38

The sites are given in Fig. 3

was predominant. Also, towards the west, the mean value of Rxz increases gradually from 1.85 to 4 over a distance of 1 km towards the Taygetos Thrust (Fig. 4a(ii), 4b(ii)). The spatial orientations of the strain ellipsoids in the X–Z and X–Y planes for the PQ series, at a distance of over 1 km from the Taygetos Thrust (Fig. 4), mainly demonstrate the NE trend of the X-axes parallel to the stretching lineation L_1.

A kinematic interpretation of our strain analyses indicates that during the D1 deformation phase, the Taygetos anticline probably acted as a barrier producing the flattening of strain ellipsoids near the Taygetos Thrust. A late increment of plane strain may have caused horizontal motion of material parallel to the thrust. Further east, where the PQ nappe moved freely westwards, prolate strain ellipsoids predominate. The NNE-trending X-axes of the strain ellipsoids at sites Xr5 and Xr6 in Fig. 4b, as well as the SSW sense of shear shown by the quartz c-axis fabric Q4, indicates that the Taygetos barrier may have been active during the D2 deformation.

Extensional structures

The Taygetos Mountain, with elevations as much as 2400 m, constitutes the footwall upland to the western marginal fault of the Sparta Graben (Fig. 5a). This fault trends nearly parallel to the eastern margin of the Taygetos window and is expressed as a steep escarpment, as much as 700 m in height, running discontinuously for 45 km along the mountain front. Dip-slip movements on the fault involving long-term rates of 1 mm/year have been activated in historical times by earthquake events of magnitude M≈7 (Armijo et al. 1991) and are responsible for the asymmetrical subsidence of the graben. The Tertiary infilling of the graben contains several hundred metres of Plio-Pleistocene sediments, including terrestrial and lacustrine facies in the north and marine facies in the south (Piper et al. 1982). In the northern part of the basin,

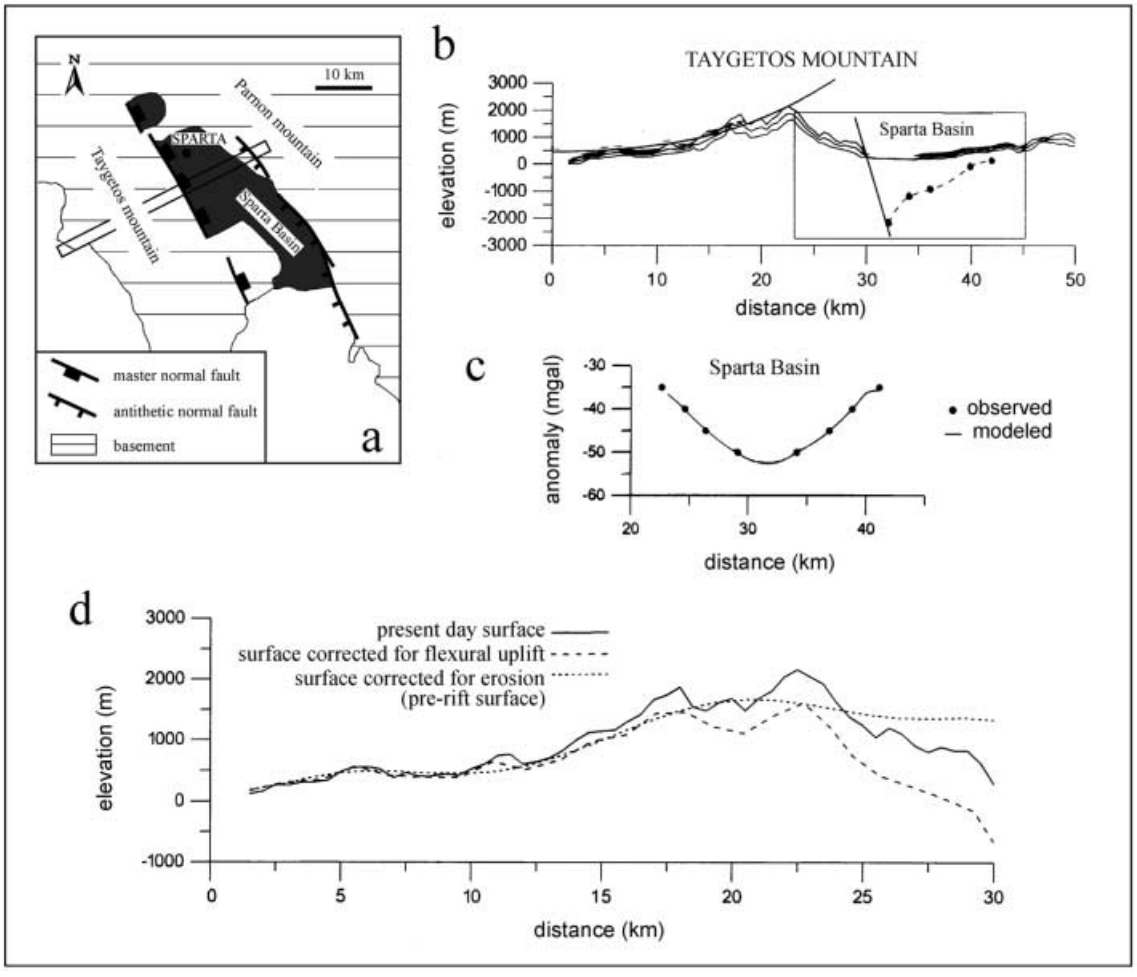

Fig. 5 **a** Summary tectonic map of the Sparta graben, showing location of the graben and shoulder mountains. Location is given in Fig. 1. The *rectangle* denotes the area for which topographic and gravity data have been projected onto the profiles. **b** Topographic profiles across the graben are interpreted to show evidence of rift flank uplift and the sediment thickness in the basin. Maximum, average and minimum elevations are shown, derived from projecting elevations within a 4-km-wide swath. **c** Bouger gravity anomaly across the basin and **d** computed model. Static model showing the landscape evolution of the Taygetos Mountain area

incorporated in our study, upper Pliocene extensive floodplain silts pass upward into lacustrine marls. They are overlain by lower Pleistocene alluvial fans and fluviatile conglomerates.

It is argued that the major factor contributing to the building of Taygetos Mountain was flexural uplift with viscoelastic relaxation resulting from the mechanical unloading of the crust during extension (Fig. 5b; Poulimenos and Doutsos 1997). The uplift mechanisms involve isostatic compensation of the loading of the Sparta basin and the erosional unloading of the mountain front. A thermal uplift mechanism seems highly unlikely because the invoked flexural models constrain the elastic thickness to 15 km suggesting compensation within a viscous lower crust rather than the thermal lithosphere. In this section we attempt to remove the isostatically driven effects in order to resolve the pre-rift elevation profile of the Taygetos Mountain. This procedure is based on the available geological data and provides a rough mechanical interpretation, which can, however, be included in the pre- rift assessment. The used physical constants are presented in Table 2.

As the first step in this exercise we determined the basin load which was defined as the amount of crust replaced by low-density material multiplied by the contrast in specific gravity between crust and altered material. In doing so, Bouguer gravity data (Makris 1977) were inverted to reconstruct the basin-floor geometry (Fig. 5c). The results suggest that the basin is as much as 16 km wide and reaches a maximum depth of 2.4 km (Fig. 5b). This depth, added to the fault scarp height, yields a 3-km value for the cumulative Plio-Quaternary displacement along the marginal fault giving an inferred average slip rate of 1 mm/year, a reasonable hypothesis. Approximating the basin geometry by a triangular cross-sectional area of approximately 20×10^{10} m^2, the sedimentary line loading of the crust is calculated to be $\sim 5 \times 10^{10}$ N/m.

The second step requires estimation of the erosional unloading that is determined indirectly from the sedimentary fill of the basin. The volumetrically major part of the basin includes shaley sands compacted on burial. Compaction is primarily a function of depth and rock type and maintains the porosity–depth relation (Athy 1930)

$$f = f_0 e^{-cz}, \quad (1)$$

where f_0 is the surface porosity, z is depth in kilometres and c is the porosity "decay" constant with depth. Taking for the shaley sand $f_0 = 0.56$ and $c = 0.39 \times 10^{-5}$ cm^{-1} (Sclater and Christie 1980), Eq (1) yields $f \approx 0.2$ at the maximum depth of the Sparta basin, which in turn suggests a value of approximately 0.4 for the mean porosity of the entire sedimentary sequence. Recalling that the porosity is the ratio of void volume to total volume l/t, the solid volume Vs is given by:

$$Vs = Vt\ (1-f). \quad (2)$$

The solution of Eq. (2) in terms of unit volumes and for the inferred V_t/m $\cong 20 \times 10^{10}$ m^2 and $f \approx 0.4$ of the Sparta basin gives a 12×10^6 m^2 value for the cross-sectional area of the sediment grains. If the sediments were equally supplied from Taygetos Mountain on the master fault side and from Parnon mountain on the antithetic fault side (Fig. 5a), then the basement rocks eroded from the Taygeros escarpment approximate a cross-sectional area of 6×10^6 m^2; the latter suggests an equivalent line load of $\approx 1.5 \times 10^{11}$ N/m.

Therefore, it is demonstrated that the total load responsible for the flexural isostatic rebound of the Taygetos Mountain amounts to $\approx 2 \times 10^{11}$ N/m. The deflection profile due to this loading is calculated numerically based on a 15-km-thick viscoelastic crustal plate flexurally uplifted for 3.2×10^6 years. For brevity we did not reproduce the mathematics for the deflection calculations; the interested reader is referred to Zandt and Owens (1980) and McNutt (1980) for derivations. The calculated flexure curve indicates that the isostatically induced uplift increases towards the marginal fault to a maximum value of 1 km. By subtracting the inferred uplift estimates from the present topography, we can assess the pre-rift morphology of the Taygetos Mountain, by taking into account, however, the erosional effect (Fig. 5d, dotted line). We approximate the missing eroded area of 6×10^6 m^2 by a triangular cross section. The result illustrates a flat-line morphology stepped down almost 1000 m 15 km away from the graben (Fig. 5d, dashed line). Another way to estimate the footwall uplift along the Sparta fault is to consider displacements along seismogenic faults of similar kinematics. Geodetic measurements on comparably seismogenic faults in the north Peloponnesus indicate a subsidence/uplift ratio of approximately 2 (Koukouvelas and Doutsos 1996). Thus, the hangingwall subsidence along the Sparta fault of approximately 2.5 km may indicate a footwall uplift of approximately 1250 m.

Table 2 Physical constants used in this paper

Parameter	Value
Density of sedimentary fill	2450 kg/m^3
Crust density	2700 kg/m^3
Substratum density	2900 kg/m^3
Gravitational acceleration	9.8 m/s^2

Kinematics of the Taygetos window

The PLK in the core of the Taygetos window lies in a westward overturned anticline, formed after the Early Oligocene under ductile conditions and acted as a major obstacle to the westward-directed movements taking place along the Taygetos Thrust. Carrying PQ rocks, this thrust is a crustal-scale ramp along which

rocks were continuously deformed and uplifted from deeper structural levels, characterized by blueschist facies metamorphism (D1 phase), to higher structural levels, characterized by brittle–ductile conditions (D2 phase, backthrusting). D1 and D2 mesoscopic folds within the PLK were not rotated into parallelism during the ENE-directed nappe movements that affected the PQ series. All these structural characteristics support autochthony of the PLK. During these forward- and backward-directed thrust movements a huge mass of rock must have been eliminated from the area of Taygetos Mountain (see Discussion), because further east in the Sparta basin Pliocene sediments were deposited directly above the Kastania phyllites.

Extension along the reactivated eastern margin of the Taygetos window formed the Sparta normal fault. Taygetos Mountain has been uplifted approximately 1200 m in the footwall of the Sparta fault. The maximum downthrow movements along this fault occur only where the Taygetos Thrust dips moderately to the east. Further south, where the Taygetos Thrust gradually becomes a backthrust, the relative downthrow along the Sparta fault diminishes rapidly.

The Parnon window

Contractional structures

The Parnon Window is a 30-km-long and up to 10-km-wide structure (Fig. 1) which is located approximately 25 km east of the Taygetos Window. Our detailed structural mapping was confined to the northern part of this window (Fig. 6). The core of this window is a west-verging, overturned anticline (Fig. 6, cross section E–E′), similar in geometry to the Taygetos anticline.

Fig. 6 Tectonic map, cross-sections and an equal-area projection from the Parnon window, location of map is given in Fig. 1

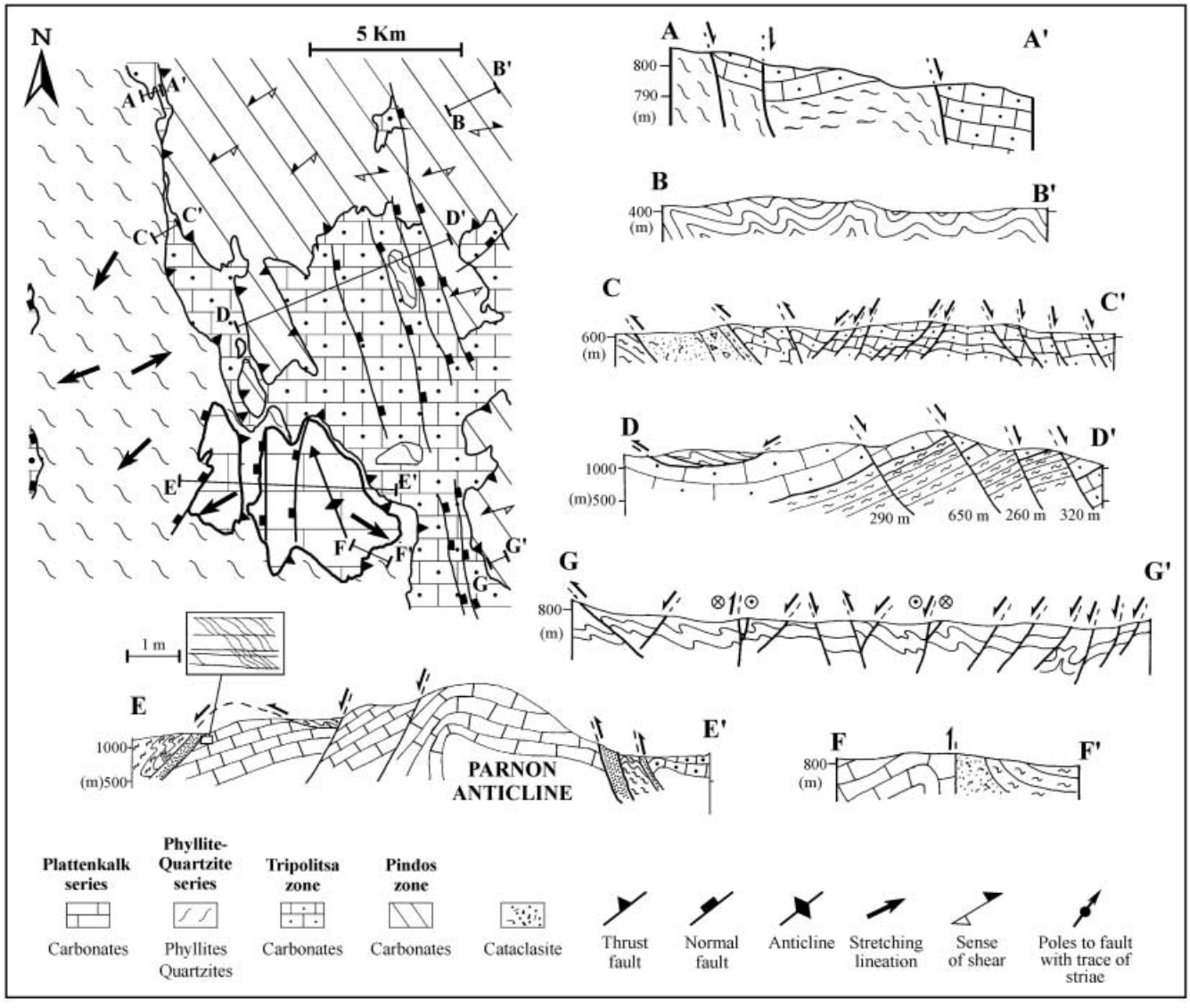

Mesoscopic folds (D1 folds) trend mainly NNW, but there are also NNE- and ENE-trending folds. The latter folds are sheath folds and often trend parallel to the stretching lineation (Fig. 6, tectonic map), which is generally most pronounced in the upper parts of the PLK. During the late stages of deformation, D2 folds are formed. These folds are kink-like in shape and are associated with a spaced cleavage, subparallel to the axial planes of the folds.

As in the Taygetos area, the contact between PLK and PQ series in the Parnon window is a crustal scale contractional ramp called "the Parnon Thrust". It is marked by cataclasites approximately 150 m thick. The thrust dips nearly vertically at the eastern margin of the window and gently westward at its western margin (Fig. 6, cross section E–E′). To the south the Parnon Thrust swings gradually to an ENE direction and is overturned dipping steeply to the NW, carrying the PLK series above the PQ series (Fig. 6, cross section F–F′). In addition, abundant D2-kink folds and associated backthrusts were observed at both sides of this fault suggesting overthrust movements towards the SE. The PQ series at the eastern margin of the Parnon window is extremely thinned and deformed, whereas at the western margin it displays a thickness of approximately 1000 m. Here it forms a monotonous sequence that is internally deformed by ENE-trending folds (Fig. 6, cross section E–E′) and a parallel stretching lineation.

The contact between the PQ series and the Tripolitsa limestones is a decollement zone of cataclasites up to 70 m thick (Fig. 6, cross section C–C′). In places, where the Tripolitsa limestones are thin, this zone attains a thickness of approximately 200 m (see also Dercourt 1964) and is associated with west-verging folds and shear planes indicating west-directed shearing.

Tectonically above the Tripolitsa zone is the Pindos zone, showing a different style of deformation. Rocks in the hangingwall of the Pindos Thrust are deformed by D1 structures including recumbent isoclinal folds, thrusts and a dense system of s–c brittle fractures implying a top-to-the-SW sense of movement (Fig. 6, cross section G–G′). Approximately 500 m east of the Pindos Thrust and all the way to the Aegean coast, these structures are superimposed by D2 showing no pronounced vergence. Common bivergent box folds (Fig. 6, cross section B–B′) suggest pure shear conditions with maximum extension nearly vertical.

Extensional structures

The major decollement zone between the PQ series and the Tripolitsa limestones at the eastern margin of the Parnon window is reactivated to become a normal fault. Smaller, synthetic normal faults in the hangingwall block of this fault support the movements towards the southeast. Further east (Fig. 6, cross section D–D′), the contact between PQ series and the Tripolitsa limestones can be used as a marker to estimate separation along normal faults, which is in the range of 250–650 m. Cumulative displacements along these faults has formed a structural relief in excess of 1500 m. Since no basin development and deposition of sediments has occurred in that area, the onset of extension is difficult to estimate (see Discussion).

Kinematics of the Parnon window and comparison with the Taygetos window

In general, the Parnon window shows a kinematic picture similar to that of the Taygetos window. Some structural differences, however, indicate modifications of the kinematics. For example, ENE-trending plastic folds associated with a stretching lineation within the PLK carbonates in the core of the Parnon window show that the PLK was strongly affected by the top-to-the-SW directed shearing, unlike the PLK in the Taygetos window; therefore, in this region the PLK may be allochthonous, being detached from an unknown basement by a sole thrust (see Fig. 8d). In addition, the thicker cataclasites seen along the Parnon Thrust may indicate faster overthrusting of the PQ above the PLK (see Discussion).

The Taygetos and the Parnon thrusts both show a similar geometry and gradually develop into backthrusts to the south. Although both faults were reactivated during their late orogenic evolution into normal faults, the cumulative vertical displacements in the Parnon window area are smaller and no basin development and deposition of sediments has occurred.

The Molai area

In the Molai area (Fig. 7a) competent, basal limestones of the Tripolitsa zone pass westwards at Kourkoula Mountain area into incompetent thin limestones and schists underlain by the Tyros beds (Fig. 7b; see also Doutsos and Koukouvelas 1985). The Molai area is a transition zone showing a significant change in the deformational style from east to west. To the east, west-facing normal faults cut the Tripolitsa carbonates, but to the west at the Kourkoula Mountain west-verging isoclinal folds and an ENE-trending stretching lineation deform the Tripolitsa limestones. These structural data allow us to assume that most of the observed normal faults within the Tripolitsa zone are produced by the westward-directed regional shearing. A large arcuate backthrust, the Molai Thrust, carries the thin marbles and schists of the Kourkoula series eastwards above the Tyros beds (Fig. 7, cross section A–A′ and B–B′). Parallel to this thrust trend is the Molai basin, an extensional asymmetrical basin formed during the late Neogene (Brauer 1983; Tavitian 1994).

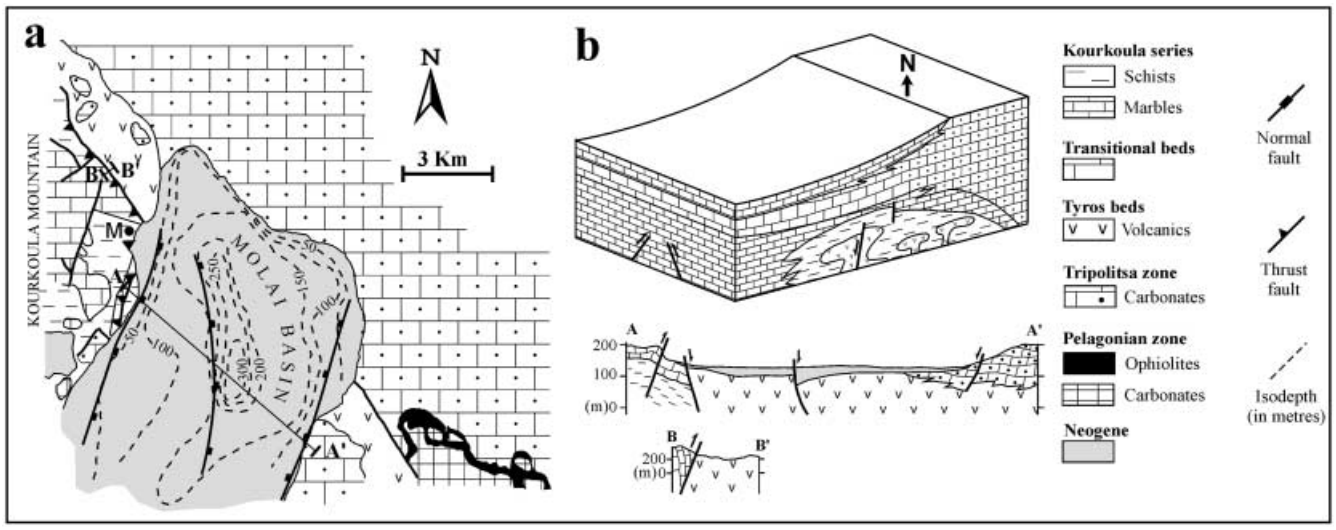

Fig. 7 **a** Tectonic map and cross sections of the Molai area. Location of map is given in Fig. 1. **b** Diagram shows the three-dimensional relationship between Tripolitsa zone and Kourkoula series

Cumulative vertical movements along the east-facing normal faults of this basin are approximately 500 m.

Discussion and conclusion

Plate collision and exhumation history of the tectonic windows in the south Peloponnesus are reconstructed by combining our structural data with the stratigraphic records of the basins which have developed on the Apulian microcontinent.

Pre-collisional stage

A rifting during Triassic and Jurassic times divided the Apulian microcontinent into several palaeogeographic realms, including the Pindos passive continental margin to the east, the deep basins of the Ionian zone and PLK series to the west and a shallow platform (Tripolitsa zone) to a central domain (Fig. 8a). In our interpretation the PLK series represents the southern prolongation of the Ionian zone, whereas the PQ series is a Permian–Middle Triassic rift sequence which was later metamorphosed under blueschist-facies conditions. In some places, such as in the Molai area, this sequence grades upward into thin marbles, which can be considered to be the transition between the PLK and the Tripolitsa carbonates.

Syn-collisional stage

In the late Eocene, the Pelagonian and Apulian microcontinents were involved in convergent tectonics, whereas the Pindos ocean subducted eastwards (Fig. 8b). During this stage the Pindos rocks overthrusted westwards onto the Tripolitsa limestones. As a result, the Apulian margin thickened, uplifted and subdivided in synorogenic flysch basins, which were formed by southwest progradation of thrusting and folding. The early Oligocene underplating of the Apulian below the Pelagonian microcontinent resulted in the westward obduction of the ophiolitic rocks over the Pindos flysch. Later in the upper Oligocene, continental subduction along the Pelagonian margin was hindered and convergence continued further to the west along the boundary between Tripolitsa carbonates and the PQ series protolith. In the course of this tectonism, the protolith of the PQ series might have been tectonically buried to a depth of 45 km, in order to have experienced pressures over 13 kbar (Fig. 2; Theye 1988; Theye and Seidel 1991).

The exhumation history of the deeper parts of the orogen began at the Oligocene–Miocene boundary (~24 My; Figs. 2, 8c). The PQ series started to extrude between the Parnon Thrust and the basement of the Tripolitsa carbonates. The effect of this extrusion was to place the metamorphosed rocks of the PQ series in contact with the overlying unmetamorphosed Tripolitsa carbonates along a normal fault but in a tectonic setting without any net extension of the overall system (Fig. 8c). Recent work, in the Alps and in the Franciscan complex, emphasizes that this tectonic regime can be explained if we accept a reduction of the negative slab load which acts and flexes the slab upward (Ernst and Liou 1995; Escher and Beaumont 1997). In the south Peloponnesus this increased buoyancy in the continental subduction zone may be produced by the progressive entrance of the low-density continental crust and the PLK carbonates in the subduction zone. The ENE-trending and gently plunging X-axes of prolate strain ellipsoids, combined with the top-to-the-SSW sense of shear of the c-axis fabrics and the occurrence of plastic s-type folds, appears to indicate extrusion of the PQ series to the southwest.

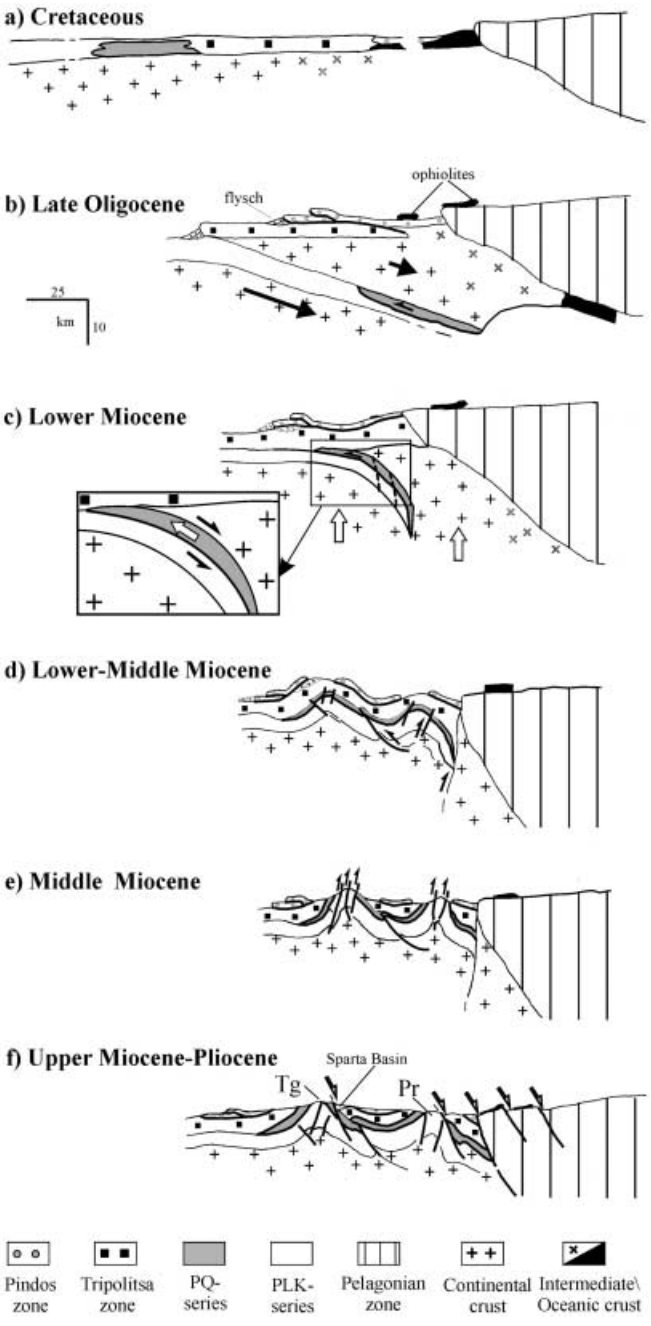

Fig. 8a–f Suggested evolutionary model of development of the south Peloponnesus along a cross section through Parnon (*Pr*) and Taygetos (*Tg*) Mountains (see text for explanations)

The late stage of this horizontal extrusion was marked by the establishment of the Taygetos and Parnon anticlines, which acted as pediments inhibiting the west-directed movements (Fig. 8d). The rapid extrusion seems to end at 19 My as the rocks reached the depth of 10 km (Thomson et al. 1998). Taking into account that rocks during extrusion uplifted from 45 to 10 km depth in the time interval between 24 and 19 My, we estimate an average exhumation rate of the order of 7 mm/year.

Post-collisional stage

As the deformation continued in the lower Miocene time (D2 deformation), the Taygetos and Parnon anticlines were tightened and the Taygetos and the Parnon thrusts rotated backwards (Fig. 8d,e). In the same time flysch basins on the Tripolitsa nappe continued to develop in a piggy-back style simultaneously with southwest thrusting (Richter 1976). It seems that contractional movements lasted until the middle Miocene, as in the case of the molassic basins further east in the internal Hellenides, i.e. Mesohellenic Trough (Doutsos et al. 1993), Cyclades (Boronkay and Doutsos 1994) and Crete (Postma and Drinia 1993; Kokkalas and Doutsos, in press). Early late Miocene clastic deposits in the Kythira island, which rest uncomformably on the PQ series (Meulenkamp et al. 1977), give the upper stratigraphic bracket of the syncompressional uplift and exhumation in this area. Therefore, we conclude that during the D2 deformation rocks were exhumed from a depth of 10 km in the time space between 19 and 13 My, giving exhumation/denudation rates of the order of 1.5 mm/year.

Late-collisional stage

Late orogenic sedimentation in the south Peloponnesus involved the deposition of coarse non-marine clastics in small isolated basins. These deposits underlie Pliocene marls and clays and overlie Cretaceous limestones of the Pindos zone and the PQ series, in the Pylos and Sparta area, respectively. If we accept an upper Miocene age for these sediments, it seems probable that large parts of the Pindos and Tripolitsa nappes were eroded during this time.

In the Plio-Pleistocene time hinterland-dipping normal faults formed large extensional basins, at the eastern margin of the Taygetos window (Fig. 8f). Footwall uplift of these normal faults do not exceed 1200 m; therefore, uplift rates are of the order of 0.2 mm/year.

In summary, the exhumation history of the metamorphic rocks in the south Peloponnesus was characterized by crustal southwest-directed simple shear in lower structural levels, which was modified by pure shear conditions in the upper structural levels later. This syncompressional exhumation was taking place during the lower Miocene with decreasing rates from 7 to 1.5 mm/year. On the other hand, the uplift rate caused by the footwall uplift in crustal scale normal faults was very slow, of the order of 0.2 mm/year.

Acknowledgements We thank G. Kowalczyk, University of Frankfurt, for helpful discussions on the stratigraphy of the southern Peloponnesus. Reviews and very helpful comments by G. Viele, University of Missouri, on a previous version of this paper are gratefully acknowledged. The paper was greatly improved by critical reviews and comments by A. Henk and an anonymous reviewer.

References

Armijo R, Lyon-Caen H, Papanastasiou D (1991) A possible normal-fault rupture for the 464 BC Sparta earthquake. Nature 351 : 137–139

Athy LF (1930) Density porosity and compaction of sedimentary rocks. AAPG Bull 14 : 1–24

Aubouin J (1959) Contribution a l'etude geologique de la Grece septentrionale: le confins de l'Epire et de la Thessalie. Ann Geol Pays Hellen 10 : 1–484

Bassias Y (1989) Paleogeographie jurassique des "Plattenkalk" ioniens dans le Peloponnese oriental (Parnon) Grece. C R Acad Sci Paris 309 : 275–281

Bassias I, Thiebault F (1985) Les "plattenkalk" du Parnon (Peloponnese oriental Grece): confirmation de leur rattachement a la zone ionienne; donnees preliminaires sur leurs caracteristiques structurales et metamorphiques. Bull Soc Geol France 8 : 495–501

Bernoulli D, Renz O (1970) Jurassic carbonate facies and new ammonite faunas from western Greece. Eclogae Geol Helv 63 : 573–607

Bizon G, Thiebault F (1974) Donnees nouvelles sur l'age des marbres et quartzites du Taygete (Peloponnese meridional Grece). C R Acad Sci Paris 278 : 9–12

Blumor T (1998) Die Phyllit-Qyarzit-Serie SE-Lakoniens (Peloponnes, Griechenland): Hochdruckmetamorphite in einem orogenen Keil. Frankfurter Geowiss Abh 17 : 1–190

Blumor T, Dollinger J, Knobel M, Mutter A, Zarda S, Kowalczyk G (1994) Plattenkalk series and Kastania phyllites of the Taygetos Mts.: new results on structure and succession. Bull Geol Soc Greece 15 : 83–92

Bonneau M (1973) Sur les affinites ioniennes des "calcaires en plaquettes" epimetamorphiques de la Crete le chariage de la serie de Gavrovo-Tripolitza et la structure de l'arc egeen. C R Acad Sci Paris 277 : 2453–2456

Boronkay K, Doutsos T (1994) Transpression and transtension within different structural levels in the central Aegean region. J Struct Geol 16 : 1555–1573

Brauer R (1983) Das Praneogen im Raum Molaoi-Talanta/SE-Lakonien (Peloponnes Griechenland). Frankfurter Geowiss Abh 3 : 1–300

Burchfiel BC, Royden LH (1985) North–south extension within the convergent Himalayan region. Geology 13 : 679–682

Clift PR (1992) The collision tectonics of the southern Greek Neotethys. Geol Rundsch 81 : 669–679

Davis GH, Coney PJ (1979) Geologic development of the Cordilleran metamorphic core complexes. Geology 7 : 120–124

Dercourt J (1964) Contribution a l'etude geologique d'un secteur du Peloponnese septentrional. Ann Geol Pays Hellen 15 : 1–418

Dewey JF (1988) Extensional collapse of orogens. Tectonics 7 : 1123–1139

Dittmar U, Kowalczyk G (1989) Das Liegende der Plattenkalk-Karbonate im Taygetos (Sud Peloponnes). Nachrichten Deutsch Geol Gesellschaft 41 : 88–89

Doert U, Kowalczyk G, Kauffmann G, Krahl J (1985) Zur stratigraphischen Einstufung der "Phyllit-Serie" von Krokee und der Halbinsel Xyli (Lakonien Peloponnes) Erlanger Geol Abh 112 : 1–10

Doutsos T, Koukouvelas I (1985) Structurelle Entwicklung des Pb- Zn- Cu- Ag- Vorkommens von Molai (Sudpeloponnes). Min Wealth 40 : 7–16

Doutsos T, Piper G, Boronkay K, Koukouvelas I (1993) Kinematics of the Central Hellenides. Tectonics 12 : 936–953

Doutsos T, Koukouvelas I, Zelilidas A, Kontopoulos N (1994) Intracontinental wedging and post-orogenic collapse in the Mesohellenic Trough. Geol Rundsch 83 : 257–275

Dunne WM, Onash CM, Williams RT (1990) The problem of strain marker centers and the Fry method. J Struct Geol 12 : 933–938

Dunnet D (1969) A technique of finite-strain analysis using elliptical particles. Tectonophysics 7 : 117–136

England P, Molnar P (1990) Surface uplift, uplift of rocks and exhumation of rocks. Geology 18 : 1173–1177

Ernst WG, Liou JG (1995) Contracting plate-tectonic styles of Quinling-Darbie-Solou and Franciscan metamorphic belts. Geology 23 : 353–356

Erslev EA (1988) Normalized center-to-center strain analysis of packed aggregates. J Struct Geol 10 : 201–209

Erslev EA, Ge H (1990) Least-squares center-to-center and mean object ellipse fabric analysis. J Struct Geol 12 : 1047–1059

Escher A, Beaumont C (1997) Formation, burial and exhumation of basement nappes at crustal scale: a geometric model based on the Western Swiss-Italian Alps. J Struct Geol 19 : 955–974

Etchecopar A, Vasseur G (1987) A 3-D kinematic model of fabric development in polycrystalline aggregates: comparisons with experimental and natural examples. J Struct Geol 9 : 705–717

Fry N (1979) Random point distributions and strain measurement in rocks. Tectonophysics 60 : 89–105

Fytrolakis N (1971) Die bis heute unbekannten palaozoischen Schichten sudostlich von Kalamata. Bull Geol Soc Greece 8 : 70–81

Gerolymatos I (1994) Metamorphose und Tectonik der Phyllit-Quartzit-Serie und der Tyros-Schichten auf dem Peloponnes und Kythira. Berliner Geowiss Abh (A) 164 : 1–101

Hossack JR (1968) Pebble deformation and thrusting in the Bygdin area (S Norway). Tectonophysics 5 : 315–319

Hsu KJ (1991) Exhumation of high-pressure metamorphic rocks. Geology 19 : 107–110

Jacobshagen V (1986) Geologie von Griechenland. Borntraeger, Berlin, pp 1–363

Jacobshagen V (1994) Orogenic evolution of the Hellenides: new aspects. Geol Rundsch 83 : 249–256

Jacobshagen V, Durr S, Kockel F, Kopp KO, Kowalczyk G, Berckheimer H, Buttner D (1978) Structure and evolution of the Aegean Region. In: Closs H, Roeder D, Schmidt K (eds) Alps Apennines Hellenides. Schweizerbart, Stuttgart, pp 537–564

Jensen LN (1984) Quartz microfabric of the Laxfordian Canisp Shear Zone NW Scotland. J Struct Geol 6 : 293–303

Karakitsios V (1995) The influence of preexisting structure and halokinesis on organic matter preservation and thrust system evolution in the Ionian Basin, Northwest Greece. AAPG Bull 79 : 960–980

Katagas C (1980) Ferroglaucophan and chloritoid-bearing metapelites from the phyllite series southern Peloponnese Greece. Mineral Mag 43 : 975–978

Kokkalas S, Doutsos T (in press) Strain partitioning along the south Hellenides (eastern Crete, Greece). In: Panayides I, Xenophontos C (eds) Third International Conference on the geology of the Eastern Mediterranean, Geological Survey Department, Nicosia, Cyprus

Kowalczyk G, Zugel P (1997) Die Vathia-Schichten – Flysch der Plattenkalk-Serie des Peloponnes. Kontribution Forschungen Institut Senckenberg (in press)

Kowalczyk G, Richter D, Risch H, Winter P (1977) Contribution to the tectogenesis on the Peloponnesus (Greece). N Jahrb Geol Paläont Mh 1977 : 549–564

Koukouvelas IK, Doutsos T (1996) Implications of structural segmentation during earthquakes: the 1995 Egion earthquake Gulf of Corinth Greece. J Struct Geol 18 : 1381–1388

Ktenas KA (1924) Formations primaires semimetamorphiques au Peloponnese central. CRS Soc Geol France 24 : 61–63

Lallemant S (1984) La transversale nord-maniote Etude geologique et aeromagnetique d'une structure transverse a l'arc egeen externe (These 3′ cycle University Pierre et Marie Curie). Sci Terre Mem Paris 84 : 1–164

Law RD (1987) Heterogeneous deformation and quartz crystallographic fabric transitions: natural examples from the Stack of Glencoul northern Assynt. J Struct Geol 9 : 819–833
Lisle RJ (1985) Geological strain analysis: a manual for the R_f/φ method. Pergamon Press, New York, pp 1–99
Lister GS, Hobbs BE (1980) The simulation of fabric development during plastic deformation and its application to quartzite: the influence of deformation history. J Struct Geol 2 : 355–370
Lister GS, Banga G, Feenstra A (1984) Metamorphic core complexes of Cordilleran type in the Cyclades Aegean Sea Greece. Geology 12 : 221–225
Makris J (1977) Geophysical investigations of the Hellenides. Hamb geophys Einzelschriften 34 : 1–124
Manutsoglu M (1990) Tectonic und Metamorphose der Plattenkalk-Serie im Taygetos (Peloponnes Griechenland). Berliner Geowissen Abh 129 : 1–82
McNutt M (1980) Implications of regional gravity for state of stress in the Earth's crust and upper mantle. J Geophys Res 85 : 6377–6396
Merle O, Guillier B (1989) The building of the Swiss Central Alps: an experimental approach. Tectonophysics 165 : 41–56
Meulenkamp J, Theodoropoulos P, Tsapralis V (1977) Remarks on the Neogene of Kythira, Greece. Sixth Coll Geol Aegean Region 1 : 355–362
Panagos AG, Pe-Piper GG, Piper DJW, Kotopouli CN (1979) Age and stratigraphic subdivision of the Phyllite series Krokee region Peloponnese Greece. N Jahrb Geol Paläont Mh 1979 : 181–190
Paraskevopoulos G (1964) Die alpine Dislokationsmetsmorphose im zentral peloponnesisch-kretischen metamorphen system. N Jahrb Min Abh 101 : 195–209
Pe-Piper GG (1982) Geochemistry tectonic setting and metamorphism of mid-Triassic volcanic rocks of Greece. Tectonophysics 85 : 253–272
Philippson A (1892) Der Peloponnes Versuch eine Landeskunde auf geologischer Grundlage. Friedlander, Berlin, pp 1–642
Piper DJW, Pe-Piper GG, Kontopoulos N, Panagos AG (1982) Plio-Pleistocene sedimentation in the western Lakonia graben Greece. N Jahrb Geol Paläont Mh 1982 : 679–691
Platt JP (1986) Dynamics of orogenic wedges and the uplift of high-pressure metamorphic rocks. Geol Soc Am Bull 97 : 1037–1053
Platt JP, Behrmann JH (1986) Structures and fabrics in a crustal scale shear zone Betic Cordilleras SE Spain. J Struct Geol 8 : 15–34
Postma G, Drinia H (1993) Architecture and sedimentary facies evolution of a marine expanding outer-arc half-graben (Crete late Miocene). Basin Res 5 : 103–124
Poulimenos G, Doutsos T (1997) Flexural uplift of rift flanks in central Greece. Tectonics 16 : 912–923
Psonis K (1981) Presence of Permo(?) Lower Triassic beds at the base of Plattenkalk series in Taygetos Description of a continuous section. Ann Geol Pays Hellen 30 : 578–587
Ramsay JG (1967) Folding and fracturing of rocks. McGraw-Hill, New York, pp 1–568
Ramsay JG, Huber MI (1983) The techniques of modern structural geology, vol 1. Strain analysis. Academic Press, New York, pp 1–307
Ratschbacher L, Frisch W, Linzer HG (1991) Lateral extrusion in the Eastern Alps. Part 2. Structural analysis. Tectonics 10 : 257–271
Richter D (1976) Das Flysch-Stadium der Helleniden-Ein Uberblick Z Dtsch Geol Gesellschaft 127 : 467–483
Ring U (1992) The kinematic history of the Pennine nappes east of the Lepontine dome: implications for the tectonic evolution of the Central Alps. Tectonics 11 : 1139–1158
Schmid SM (1982) Microfabric studies as indicators of deformation mechanisms and flow laws operative in mountain building. In: Hsu KJ (ed) Mountain buildings processes. Academic Press, London, pp 95–110
Schmid SM, Casey M (1986) Complete fabric analysis of some commonly observed quartz c-axis patterns. Am Geophys Union Geophys Monogr 36 : 263–286
Sclater JG, Christie PAF (1980) Continental stretching: an explanation of the post-Mid-Cretaceous subsidence of the central North Sea Basin. J Geophys Res 85 : 3711–3739
Seidel E (1978) Zur Petrologie der Phyllit–Quarzit–Serie Kretas. Habit-Schr Tech Univ, Braunschweig, pp 1–145
Seidel E, Kreuzer H, Harre W (1982) A late Oligocene/Early Miocene high-pressure belt in the external Hellenides. Geol Jahrb E23 : 165–206
Simpson C, Schmid SM (1983) An evaluation of criteria to deduce the sense of movement in sheared rocks. Geol Soc Am Bull 94 : 1281–1288
Stockhert B, Wachmann M, Schwarz S (1995) Structural evolution and rheology of high-pressure/low-temperature metamorphic rocks. Bochum Geol Geotech Arbeit 44 : 235–242
Suess E (1904) Sur la nature des charriages. C R Acad Sci Paris 139 : 714–716
Tataris A, Maragoudakis N (1970) Geological map of Greece Astros sheet (1 : 50,000). IGSR, Athens
Tavitian CJ (1994) Structure and sedimentology of the Molai basin, SE Peloponnese, Greece. Mineral Wealth 90 : 25–44
Temple PG (1968) Mechanics of large-scale gravity sliding in the Greek Peloponnesos. Geol Soc Am Bull 79 : 687–700
Theye T (1988) Aufsteigende Hochdruckmetamorphose in Sedimenten der Phyllit–Quarzit–Einheit Kretas und des Peloponnes. Dissertation, Tech Univ, Braunschweig, pp 1–224
Theye T, Seidel E (1991) Petrology of low-grade high pressure metapelites from the External Hellenides (Crete Peloponnese): a case study with attention to sodic minerals. Eur J Mineral 3 : 343–366
Thiebault F (1982) Evolution geodynamique des Hellenides externes en Peloponnese meridional (Greece). Ann Soc Geol Nd 6 : 1–574
Thiebault F, Triboulet T (1984) Alpine metamorphism and deformation in Phyllite nappes (external Hellenides southern Peloponnesus Greece): geodynamic implication. J Geol 92 : 185–199
Thiebault F, Zaninetti L (1974) Sur 1'existence d'un Trias calcaro-dolomitique dans le massif du Taygete Peloponnese meridional Grece. C R Acad Sci Paris 278 : 581–583
Thomson SN, Stockhert B, Rauche H, Brix MR (1998) Thermochronology of the high-pressure metamorphic rocks of Crete, Greece: implications for the speed of tectonic processes. Geology 26 : 259–262
Wallis SR, Platt JP, Knott SD (1993) Recognition of syn-convergence extension in accretionary wedges with examples from the Calabrian arc and the eastern Alps. Am J Sci 293 : 463–495
Wernicke B, Axen GJ, Snow JK (1988) Basin and Range extensional tectonics at the latitude of Las Vegas Nevada. Geol Soc Am Bull 100 : 1738–1757
Wunderlich HG (1966) Wesen und ursachen der gebirgsbildung. Hochschultaschenbucher-Verlag, Mannheim, pp 1–367
Zandt G, Owens G (1980) Crustal flexure associated with normal faulting and implications for seismicity along the Wasatch front Utah. Seis Soc Am Bull 70 : 1501–1520